J Solid State Electrochem (2005) 9: 850–858
DOI 10.1007/s10008-005-0026-6

ORIGINAL PAPER

Paula Cojocaru · Antonello Vicenzo
Pietro Luigi Cavallotti

Electrodeposition of Au/nanosized diamond composite coatings

Received: 14 May 2005 / Revised: 24 May 2005 / Accepted: 2 June 2005 / Published online: 28 July 2005

Abstract Ultra-dispersed diamond UDD particles were codeposited in gold matrix coatings from a sulphite electrolyte, changing bath load and key operating parameters. The influence of electrolyte pH, current density and bath load on current efficiency, particle co-deposition, surface morphology and microhardness of composite coatings was investigated. UDD incorporation is mainly affected by bath load; however, particle embedding is specifically sensitive to electrolyte pH and deposition current density. The maximum mass fraction of carbon in the coating, about 0.55%, is obtained by depositing from ultrasonically pre-treated electrolytes with UDD concentration 20 g l^{-1}, pH 9.5 and 3 mA cm^{-2} . Au/UDD composites are characterised by an increased microhardness and improved wear resistance. When compared to pure gold coatings which are notoriously weak, Au/UDD electrodeposits from sulphite electrolytes represent a significant improvement.

Keywords Electrodeposition · Composite · Gold coatings · UDD · Nanosized diamond

Introduction

Metal matrix composite prepared by either electrochemical or autocatalytic deposition have been in use in industrial practice since the 1980s as wear resistant or self-lubricating coatings [1, 2]. The potential of electrocodeposition for other applications is still scarcely developed, probably also because of the peculiar intricacy of the deposition processes, which still call for in depth basic investigation in order to achieve the maturity required for industrial exploitation. Process design and characterization must consider different and dissimilar factors and facing specific problems [3, 4]: (a) the properties of the particles, including size, shape and surface chemistry; (b) the electrolyte composition, in particular particle load and pH of the bath, and operating conditions; (c) the lack of one-way correlation between operating parameters and coatings properties, which depends on both the volume fraction of the dispersed phase and the size and distribution of particles.

Research efforts over the years, see e.g. [1, 5–9], have shown that composite coatings are characterized by an ensemble of functional properties improved with respect to the pure metal matrix, including hardness, wear resistance and corrosion behaviour. In particular, the incorporation of ceramic or other hard particles is an effective way for improving coatings' hardness and wear resistance. Hardness increase can be explained according to the Orowan mechanism of dispersion hardening [10], as long as particle size is less than 1 μm [11]. This increase depends on the interparticle distance, i.e. on the particle size and the volume fraction of the hard phase. The introduction of submicron and nano-particles give perspectives to the possibility of depositing coatings with even better mechanical and tribological properties [12–14]. However, some issues are still open: (a) the difficulty to obtain stable and monodisperse nanoparticles; (b) the clustering tendency of the particles suspension in the bath; (c) the identification of the optimal working parameters for the codeposition process.

Research in the field of gold or gold alloy matrix composites, as coatings or electroformed parts, started more than twenty years ago under the motivation of providing the industry with coatings of improved mechanical properties and thermal stability [15]. New opportunities have recently emerged in the field of electrocodeposition for advanced technology applications, such as catalytic composite coatings, sensors and micro-

Presented at the 4th Baltic Conference on Electrochemistry, Greifswald, 13–16, 2005.

P. Cojocaru · A. Vicenzo (✉) · P. L. Cavallotti
Dipartimento di Chimica Materiali Ingegneria Chimica "Giulio Natta", Politecnico di Milano, Via Mancinelli 7, Milano, Italy
E-mail: antonello.vicenzo@polimi.it
Tel.: +39-02-23993140
Fax: +39-02-23993180

systems [16]. Au and Au alloys composite plating processes studied in the frame of academic research activities are not particularly numerous and are generally aimed at the preparation of wear resistant coatings, with low and stable contact resistance for connectors application: Au/Al_2O_3 composite [17–19]; Au/TiN [20]; Au/diamond [20]; Au(Co) and Au(Ni)/PTFE [21–23]. Investigations specifically devoted to the development of electroforming processes have been carried out in the authors' laboratory since years and the following composite systems were considered: Au/BC_4 [24–26]; Au-Cu/B_4C [27, 28]; Au-Cu-Cd/B_4C [24]. Current research activities concern the electrodeposition of gold matrix composites with dispersion of UDD particles in the following referred to as Au/n-C(A4) composite coatings [29].

Experimental

Pure Au and Au/n-C(A4) coatings were prepared from a gold sulphite electrolyte with the following composition (mol l^{-1}): Au(I) 0.06; $Na_2SO_3$0.60; $C_2H_8N_2$ (ethylenediamine) 0.06; As(III) 2×10^{-4}, added as As_2O_3; Na_2HPO_4 0.07; EDTA 0.054 and pH 7.5 or 9.5. Au(I) was added to plating baths from a gold 100 g l^{-1} sulphite concentrate (Engelhard); chemicals of analytical grade and distilled water were used for bath make-up. Detonation synthesis ultradispersed diamond UDD used in the electrocodeposition tests was provided by Caspio SA, Switzerland. Details on grain size distribution of aggregates as well as chemical composition of UDD powder are available [30]. This material was characterised by X-ray diffraction (XRD) and transmission electron microscopy (TEM) analysis. NiP coated brass sheets were used as substrate and a platinised titanium mesh as anode. Electrodeposition and electrocodeposition tests were carried out at current density (c.d.) in the range 3–7 mA cm^{-2}, under mechanical stirring (200 rpm) in a 500 ml beaker. Electrocodeposition tests were carried out with UDD concentration in the range 5–20 g l^{-1}, with the exception of tests for current efficiency determination (UDD 5 to 50 g l^{-1}). The electrolyte temperature was controlled at $55 \pm 2°C$.

Linear polarization measurements were carried out maintaining unaltered the experimental set-up and operating parameters used for deposition, changing to a three-electrode configuration with a Ag/AgCl reference electrode in connection to the working electrode with a Piontelli probe [31]. The working electrode was a freshly deposited Au or Au/n-C(A4) layer from the electrolyte under study, at c.d. 3 mA cm^{-2} for 300 s. A model 273A EG&G PAR potentiostat/galvanostat was used for potentiodynamic runs at scan rate 0.5 mV s^{-1}.

Composite coatings were characterised by scanning electron microscopy (SEM) for surface morphology and microstructural examination. Carbon content in composite layers was determined by elemental analysis performed with a Fison EA 1108 CHNS-O elemental analyzer. The uncertainty interval when reported represents the range defined by the minimum and maximum values measured in elemental analysis of two pieces of the same sample.

Pure Au and composite coatings were characterised in terms of micromechanical properties. Vickers microhardness (HV) data were obtained from penetration depth-load curves by means of a FISCHERSCOPE H100 microhardness measurement system. Measurements conditions were as follows: 20 mN peak load, 10 s loading/unloading time and 5 s holding time at peak load. The reported values are the average of five measurements taken on three different samples prepared in the same conditions from the same bath. Before measurements the samples surface was carefully polished with a 1 μm diamond paste on rotating wheel.

Uni-directional sliding ball wear test were performed at normal load of 125 N and rotation speed of 100 rpm, against a 40 mm steel / DLC ball, without lubrication, at 20°C and in ambient air. The wear test time was 600 s. The volumetric material loss was determined by profilometry after completion of the wear tests. In order to compare Au and Au/n-C(A4) coatings performance, wear is expressed as a volumetric wear factor (cm^3 N^{-1} m^{-1}), calculated by dividing the total volumetric wear loss by the total sliding distance and the applied load.

Results

The UDD crystal structure is that of diamond with lattice parameter about 0.357 nm; the average particle size resulting from both XRD measurements, according to Debye-Scherrer formula, and TEM observation is about 5 nm, as shown in Fig. 1. The UDD powder, due to its very nature, is characterised by a strong tendency to form clusters and cluster aggregates [32]. In fact, preliminary electrocodeposition tests at UDD bath load in the range from 5 to 20 g l^{-1} showed that UDD particles in suspension were prone to aggregation. In order to reduce the degree of particle aggregation in solution, electrocodeposition baths were subjected to an ultrasonic treatment UST (20 kHz) for 20 min before deposition. The efficacy of the ultrasonic treatment is most clearly demonstrated by the picture in Fig. 2, where two tubes containing samples of composite plating bath with 20 g l^{-1} UDD load are displayed. After dispersing the UDD powder in the electrolyte sample by vigorous shaking, one of the samples (tube on the left) was ultrasonically treated in the same condition as applied to composite plating bath and left to settle for 30 min. A notable consequence of the ultrasonic treatment is its influence on current efficiency and particle incorporation, as discussed later.

Electrocodeposition process

Low scan linear sweep polarization curves recorded at freshly deposited Au or Au/n-C(A4) layers from bath

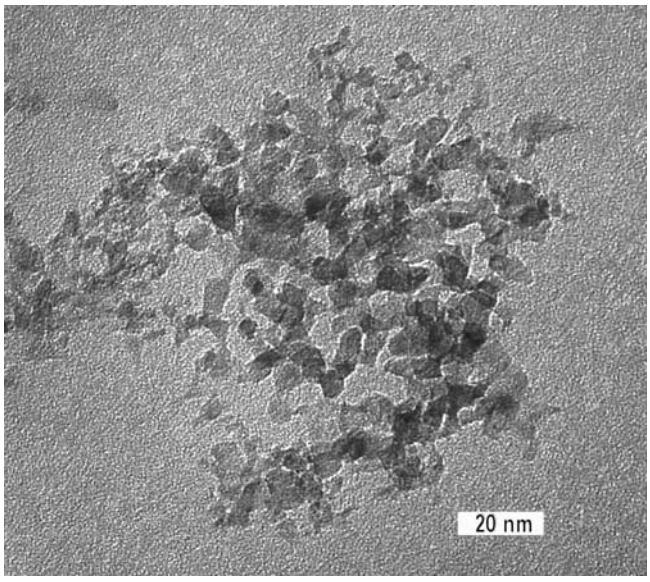

Fig. 1 TEM image of nanodiamond particles

Fig. 2 Composite plating bath samples (20 g l^{-1} UDD load) prepared by dispersing the UDD powder in the Au-sulphite electrolyte, not treated (*tube on the right*) and treated (*tube on the left*) by sonication and left to settle for 30 min

with increasing UDD particle load are presented in Fig. 3. Deposits were prepared at 3 mA cm^{-2} for 300 s from the bath under study, all other conditions being

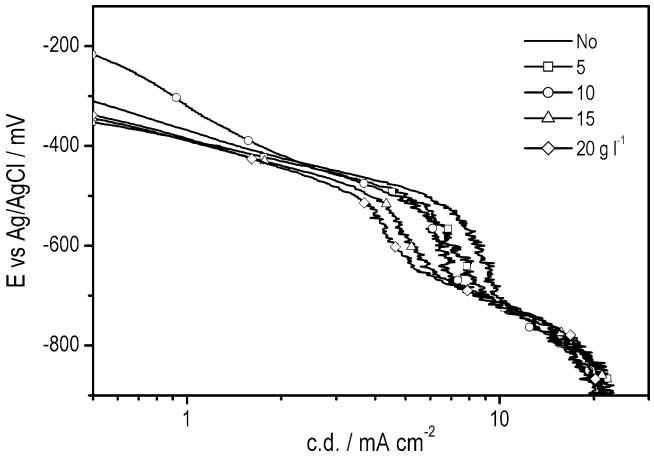

Fig. 3 Low scan (0.5 mV s^{-1}) linear polarization curves in plating bath with increasing UDD particle load at Au or Au/nC(A4) layer deposited at 3 mA cm^{-2} for 300 s from the bath under study

the same as for electrodeposition tests, as specified above.

Polarization curves in the absence of UDD particles are characterised by two well-defined waves: at lower cathodic potential, the Au(I) sulphite complex reduction takes place; at cathodic potential in excess of about −700 mV, the reduction of sulphite to dithionite ion occurs. The observed cathodic polarization behaviour is strictly comparable with early reports on the cathodic reduction of the Au(I) sulphite complex in alkaline solution [33].

At 0.5 mV s^{-1} scan rate, the main particle load sensitive feature of the polarization curves is the shift of the poorly defined current density plateau occurring in the potential range from about −500 to −700 mV, that is a decrease in c.d. as the particle load increases, for potential in the above range. This observation points out to an increase of overpotential for gold deposition in the presence of UDD particles, which is appreciated in particular at UDD load of 15–20 g l^{-1} and c.d. > 3 mA cm^{-2}, related either to a mere physical shielding of the surface or to a combined electrokinetic and shadowing effect. Polarization curves obtained at particle load of 10 g l^{-1} shows relatively low reproducibility of the potential-current density trace and displays an anodic shift of the inversion potential of up to 200 mV.

The observed trend of polarization curves can be enlightened by considering the change of current efficiency η with increasing bath load, as shown in Fig. 4 for a pH 9.5 electrolyte and 3 mA cm^{-2} deposition c.d., where error bars represent standard deviation of three measurements. Current efficiency vs. bath load follows a sigmoidal behaviour in the range 5–50 g l^{-1} . Moreover, as shown in Fig. 5, current efficiency increases with c.d. in the range from 3 to 7 mA cm^{-2} for Au/n-C(A4) composite coatings deposition. This correlation between current efficiency and c.d., depending on the electrokinetic characteristics of the sulphite electrolyte, is found to hold for both, electrolyte subjected and not-subjected

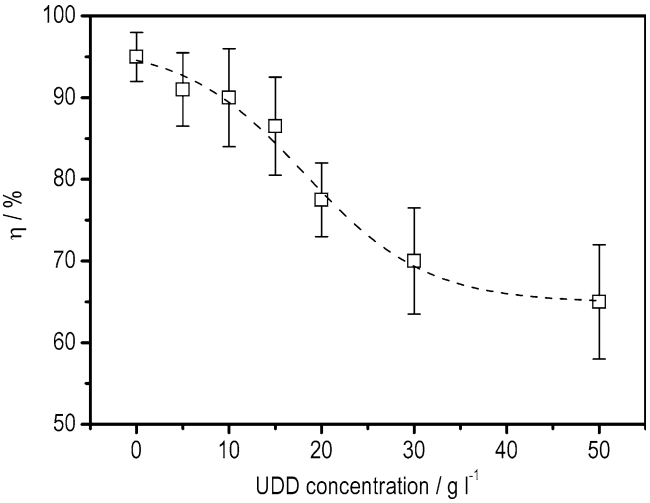

Fig. 4 Current efficiency versus UDD load in pH 9.5 Au-sulphite electrolyte (no UST; 3 mA cm^{-2}; 8.8 C cm^{-2}; 55°C; mechanical stirring 200 rpm)

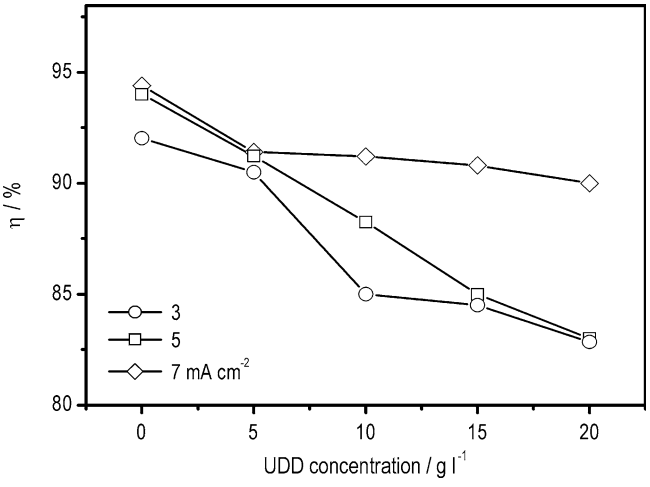

Fig. 5 Current efficiency versus UDD load for three series of electrodeposition tests from pH 9.5 Au-sulphite electrolyte (UST; 8.8 C cm^{-2}; 55°C; mechanical stirring 200 rpm). *Lines* are drawn as a guide to the eye

to UST. The observed effects of UDD load and c.d. increase on current efficiency implies that a competitive reduction process occurs in the low overpotential range and that its occurrence is kinetically enhanced by the presence of UDD. This was not investigated further in details, since it was beyond the objective of the present work.

Nanosized diamond incorporation

UDD particles incorporation in Au matrix composite coatings appears to be influenced by different factors, including bath load, ultrasonic pre-treatment of the electrolyte, pH and, to a lower extent, deposition current density. The particles load of the bath is the most important factor determining UDD particles incorporation and it is discussed in the following in conjunction with the other relevant operative factors, i.e. the UST, the deposition c.d. and the electrolyte pH.

The UST application prior to deposition was found to cause a sensible increase of both current efficiency and UDD codeposition. The current efficiency increase amounts to 5–10 percentual points, at 5 and 20 g l^{-1} bath load, respectively. The influence of UDD load on carbon content of composite coatings, depositing from electrolyte subjected and not-subjected to UST, is shown in Fig. 6. Plating conditions were as follows: pH 9.5; 3 mA cm^{-2} and 8.8 C cm^{-2}; 55°C; mechanical stirring 200 rpm. Incorporation data for electrolyte not subjected to UST are lower, do not show a defined trend and appear as less reproducible compared to data for electrolyte subjected to UST. The latter show a slight increase of current efficiency and higher level of nanosized diamond incorporation, both effects being consistent with a more finely divided form of UDD particles, if we assume that large aggregates, while not being embedded, act as a shielding obstacle lowering the surface area available for particle adsorption and gold reduction.

The type of relationship observed for UDD particles incorporation versus bath load changes with deposition c.d. in the range from 3 to 7 mA cm^{-2} as shown in Fig. 7, suggesting a quite different codeposition behaviour of UDD particles at c.d. 3 and 5–7 mA cm^{-2}. The influence of the electrolyte pH is apparently only quantitative, as shown in Fig. 8 for composite coatings prepared at c.d. 7 mA cm^{-2} from standard electrolytes at pH 7.5 and 9.5. Lowering the electrolyte pH causes a decrease of codeposited nanosized diamond particles, possibly as a consequence of surface charge modification

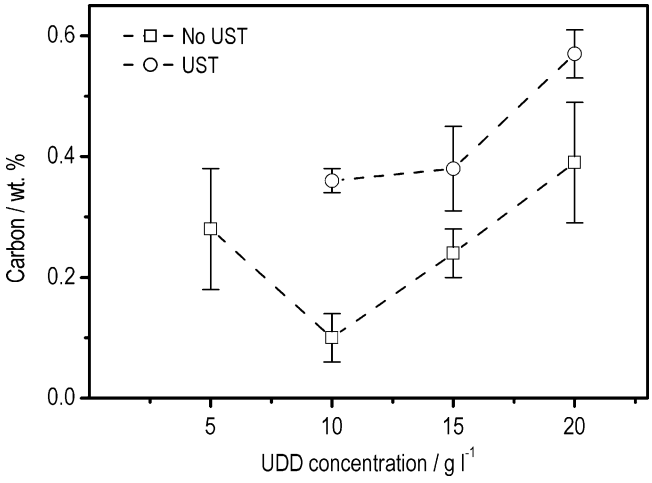

Fig. 6 Carbon content in Au/n-C(A4) composite coatings versus UDD load. Analysis were performed on two series of composite coatings prepared in the same condition (pH 9.5; 3 mA cm^{-2} and 8.8 C cm^{-2}; 55°C; mechanical stirring 200 rpm) with increasing bath load, from electrolytes subjected and not subjected to UST. *Lines* are drawn as a guide to the eye

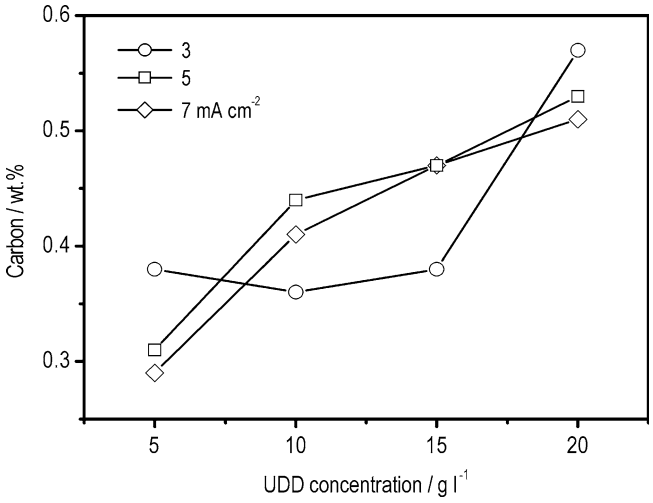

Fig. 7 Carbon content in Au/n-C(A4) composite coatings versus UDD load for different deposition current density. Operative conditions: UST; pH 9.5; 8.8 C cm^{-2}; 55°C; mechanical stirring 200 rpm. *Lines* are drawn as a guide to the eye

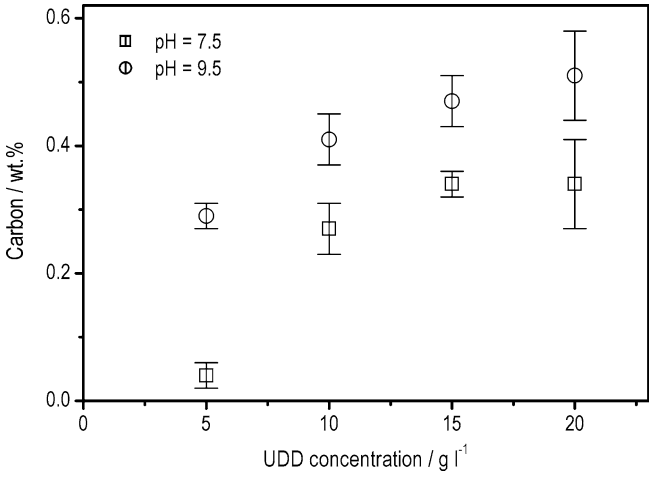

Fig. 8 Carbon content in Au/n-C(A4) composite coatings versus UDD load for pH 7.5 and 9.5 electrolytes. Data from two series of electrocodeposition tests performed in the same operative conditions: UST; 7 mA cm^{-2} and 8.8 C cm^{-2}; 55°C; mechanical stirring 200 rpm

due to changing interactions between the numerous functional groups at the surface of UDD particles, in particular hydroxyl and carbonyl groups [32], and the electrolyte species.

The surface morphology of composite coatings is, as expected, strongly affected by UDD incorporation and clearly demonstrates that particles embedding in the growing layer may occur as clusters and aggregates. SEM surface micrographs of 10 μm thick composite coatings obtained at 3 mA cm^{-2} and changing bath load from an electrolyte not subjected to UST are shown in Fig. 9. At 5 g l^{-1} UDD load, coatings present a surface marked by small pores and relatively large depressions, in which aggregates of variable size can be recognized. With UDD load increase to 10 g l^{-1}, carbon content in the coatings falls below 0.2%, the surface appears spotted with small depressions where a distinct carbon enrichment is detected by EDS. Further increasing bath load to 15 g l^{-1} shallow relatively large depressions become the dominant morphological features and particles do not emerge at the surface. At 20 g l^{-1} bath load, somewhat unexpectedly, a uniform surface texture is found, seemingly without marks and features which could be ascribed to particle embedding or shielding.

Composite coatings from electrolytes subjected to UST present quite different morphological features. The change in surface morphology with increasing thickness of composite layer, as shown by SEM surface micrographs in Fig. 10 (0.1 and 0.5 μm) and Fig. 11 (10 μm), suggests that fine UDD particles incorporated in the metal may exert a shielding effect causing the formation of pits and similar surface features or may form aggregates either with neighbouring embedded particles or as a consequence of bunching of impinging particles. In fact, with increasing thickness the surface marks of embedded particle distinctly increases in size. At 10 μm thickness, see Fig. 11, the surface is spotted with a dense array of pores, whose number and size appears related to deposition c.d. and particle incorporation.

Microhardness and wear resistance of composite coatings

In the following results on microhardness and wear resistance of Au/n-C(A4) composite coatings are presented. For composite coatings from electrolytes not subjected to UST, the relationship between surface microhardness, derived from instrumented indentation measurements, and carbon content is graphically reported in Fig. 12. The codeposition of UDD particle may have an important strengthening effect on the gold matrix; microhardness shows a clear tendency to increase as carbon content increases. However, as shown also in Fig. 12, microhardness values were found to be not very reproducible from one batch of sample to the other, i.e. series of samples prepared in the same conditions from several baths having same composition and UDD load. Microindentation characterization of composite coatings prepared from electrolytes subjected to UST is still under way; according to preliminary results, a generally lower microhardness increase is obtained, compared to the highest values observed for composite coatings from no-UST baths, and a slightly improved reproducibility.

UDD particle codeposition affects also coatings' wear resistance. The volumetric wear factor of composite coatings from electrolytes with UDD particles load 20 g l^{-1} and subjected to UST is 0.18×10^{-9} cm^3 N^{-1} m^{-1} and is remarkably lower than that for pure Au coating (0.42×10^{-9} cm^3 N^{-1} m^{-1}).

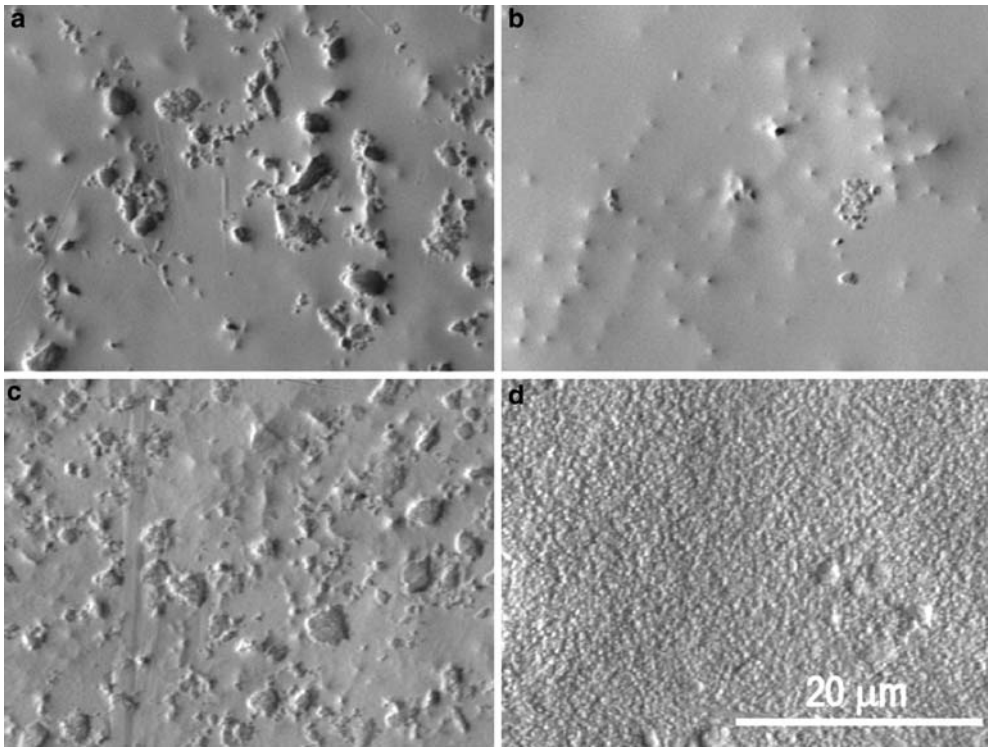

Fig. 9 SEM surface micrographs of composite coatings from electrolyte not subjected to UST obtained at 3 mA cm^{-2}, pH 9.5 and UDD bath load: **a** 5; **b** 10; **c** 15; **d** 20 g l^{-1}

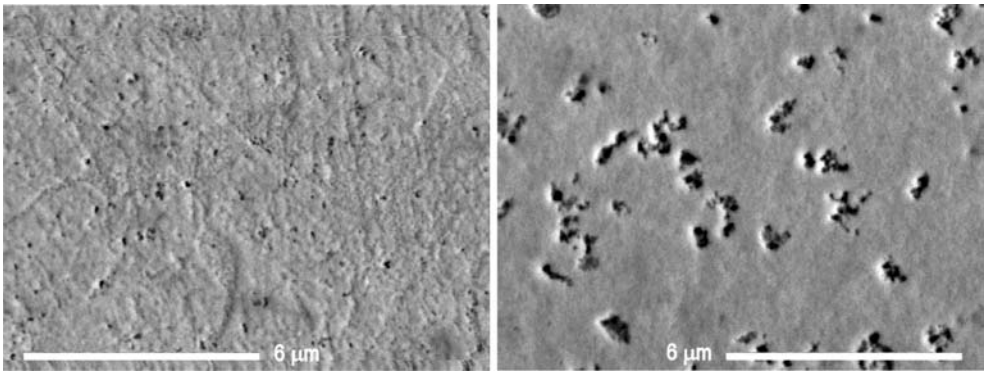

Fig. 10 SEM surface micrographs of composite coatings from electrolyte subjected to UST obtained at 3 mA cm^{-2}, pH 9.5 and UDD bath load 20 g l^{-1} ; 0.1 μm (*left*); 0.5 μm (*right*)

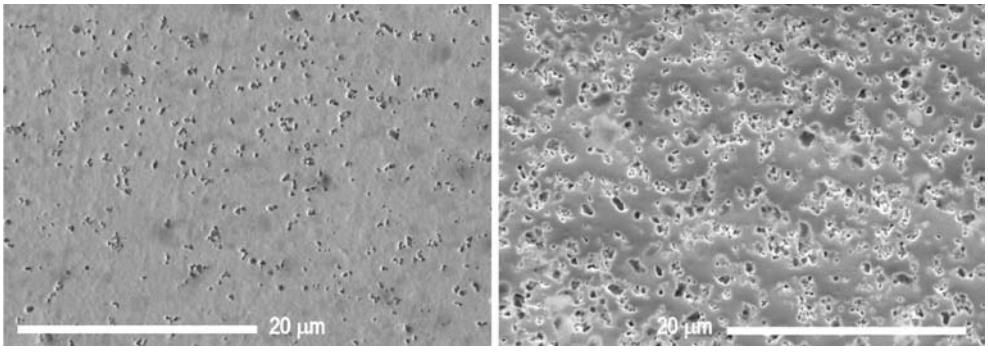

Fig. 11 SEM surface micrographs of 10 μm thick composite coatings from electrolyte subjected to UST obtained at 7 (*left*) and 3 (*right*) mA cm^{-2}, at pH 9.5 and UDD bath load 20 g l^{-1}

Discussion

There are but a few papers about the codeposition of UDD in metal matrix composite coatings by electrodeposition [32, 34–36] and detailed information about carbon content, process parameters and coatings properties is generally lacking. An extensive work appears to have been carried out by Russian researchers, but only the major achievements and the essential characteristics of coatings are known [32]. In particular, with reference to Au/n-C(A4) composite coatings, wear resistance was reported to increase by a factor of 2–5, and microh-

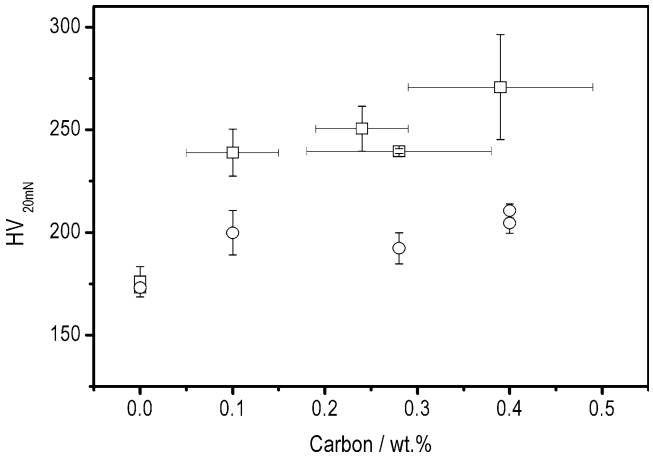

Fig. 12 Surface microhardness versus carbon mass fraction in composite coatings from electrolyte not subjected to UST obtained at 3 mA cm^{-2}, pH 9.5 and UDD bath load from 5 to 20 g l^{-1}. Two series of data are reported (denoted as *square and circle*) for deposits prepared in the same conditions from different baths having the same composition. *Y* error bar is the standard deviation of five measurements; *X* error bar is the range defined by the minimum and maximum values measured in elemental analysis of two pieces of the same sample

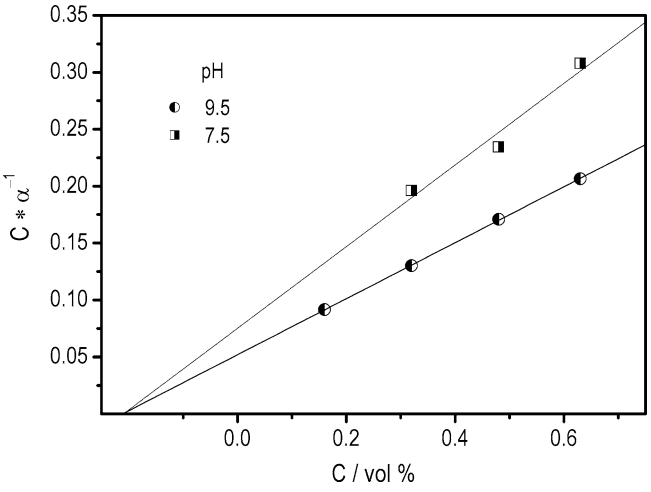

Fig. 13 Plot of $C\alpha^{-1}$ versus *C* [38] for the codeposition of UDD particles in Au matrix composite coatings, from pH 7.5 and 9.5 baths subjected to UST. Operative conditions: 7 mA cm^{-2} and 8.8 C cm^{-2}; 55°C; mechanical stirring 200 rpm. *C* is the volume fraction of particles in the bath; α is the volume fraction of particles in the composite coatings

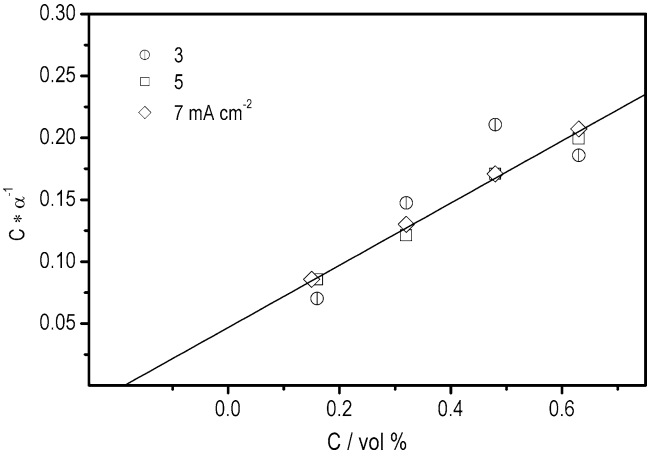

Fig. 14 Plot of $C\alpha^{-1}$ versus *C* [38] for the codeposition of UDD particles in Au matrix composite coatings, from a pH 9.5 bath subjected to UST at different deposition current density. Operative conditions: 8.8 C cm^{-2}; 55°C; mechanical stirring 200 rpm. *C* is the volume fraction of particles in the bath; α is the volume fraction of particles in the composite coatings

ardness by a factor of 1.5 compared to the Au matrix depositing from an acid gold cyanide bath [37]. Loubnin et al. carried out a detailed study on the electrodeposition of Au/n-C(A4) composite coatings from acid gold cyanide bath, reporting a maximum 1% UDD incorporation and significant improvements in microhardness and wear resistance of composite coatings compared to pure gold [36].

The relationship between UDD bath load and carbon content in the coatings was investigated in the present work, showing that UDD incorporation in the Au matrix increases with increasing bath load depending also on pH and deposition current density. Carbon mass fraction in Au/n-C(A4) composite coatings reaches a maximum of about 0.55 ± 0.05%, which, assuming a density of 3.15 g cm^{-3} for UDD [30] and of 19.3 g cm^{-3} for Au, equals a volume fraction of about 3.25 ± 0.25%. The general trend of nanodiamond incorporation vs. bath load for electrolytes subjected to UST (see Figs. 7, 8), irrespective of the pH and deposition c.d., with the exclusion of incorporation data at 3 mA cm^{-2}, recalls the codeposition behaviour first pointed out by Guglielmi for TiO_2 and SiC particles in Ni matrix composite [38]. UDD incorporation data are reported in Figs. 13 and 14 as C/α versus *C* plot in order to check the conformity of UDD incorporation to a two-steps adsorption mechanism as proposed and modelled by Guglielmi. Considering the effect of pH on UDD incorporation (Fig. 13), the agreement between incorporation data and Guglielmi's model can be considered quite good, if we admit that the slope change in the C/α versus *C* plot at changing electrolyte pH is actually related to increasing deposition overpotential as pH changes from 9.5 to 7.5. On the other hand, the influence of current density, as already pointed out, cannot be satisfactorily interpreted following the model, as pictorially shown in the graph of Fig. 14. More precisely, incorporation data at 5 and 7 mA cm^{-2} follows a common linear trend in the C/α versus *C* plot, with the same slope and intercept on the *C* axis as for data in Fig. 13 (note that incorporation data at c.d. 7 mA cm^{-2} are the same data set in both graph); incorporation data at c.d. 3 mA cm^{-2} shows a quite different codeposition behaviour.

While these results are certainly not conclusive on the mechanism of nanodiamond incorporation in Au matrix composite, they do confirm, as expected in consideration

of the chemical peculiarity of UDD clusters surface [32], that a determining factor controlling UDD codeposition is the surface adsorption interaction of the particles with the electrolyte ionic species and the growing metal surface. In fact, according to data reported in [32], the ζ potential of UDD suspension in low ionic strength aqueous KCl solution is positive in the pH range 3–11, increasing as pH increases. This is at least in qualitative agreement with the observation that UDD particles incorporation slightly increase with pH change from 7.5 to 9.5.

On the other hand, the codeposition of UDD particles is strongly affected by its tendency to agglomerate in solution and possibly also at the growing surface, as shown by the effects of UST and by the evolution of the surface morphology of composite layers with deposition time. The tendency of fine particles to agglomerate during embedding was shown by TEM examination of Ni/n-Al_2O_3 composite coatings [39].

The electrokinetic behaviour of the sulphite bath used in this work is significantly affected by the presence and codeposition of the particles, as shown by linear polarization measurements at the growing composite layer and by current efficiency change with particle concentration in the bath. The influence of the particles could be twofold: (1) a shielding effect leading to cathodic polarization and loss in current efficiency; (2) an electrokinetic catalytic effect on the cathodic reduction of sulphite to dithionite, which, under conditions of diffusion control for sulphite reduction, could explain the observed relationship between current efficiency and current density. At this stage of the investigation, these observations cannot be but speculative and further work is required for clarifying the electrokinetic characteristics of the codeposition of UDD in Au matrix composite coatings.

Despite the uncertainty on mechanism and electrokinetic behaviour, the electrodeposition of Au/n-C(A4) composite coatings was successful as long as metal matrix properties improvement is concerned. Composite layers with carbon content as low as 0.5% showed a remarkable increase in microhardness, ranging from about 210 to 250 HV compared to about 170 HV for pure Au coatings from the base electrolyte with As 30 ppm, i.e. up to 50% improvement with respect to the matrix. The microhardness increase can be attributed to a dispersion hardening mechanism of UDD particles, even if so far there is no direct evidence on size and distribution of incorporated particles. However, it may be inferred from surface morphological features that the maximum size of embedded particles and aggregates is in the range of 1 μm, i.e. the size range for which embedded particles are expected to provide dispersion hardening. This view may be further corroborated by evaluating the average number of particles per unit volume of composite material and comparing the calculated particle number density to the plastically deformed volume during indentation.

For a uniform distribution of spherical aggregates of 1 μm diameter and 3% volume fraction of carbon, the number density of codeposited particles is about 5.7×10^{10} cm^{-3}. The plastically deformed volume may be estimated from a simplified model of an elastic-plastic indentation which assumes that strains and displacements have radial symmetry with respect to the point of first contact [40]. According to this model, the radius of the plastic zone for the Au matrix may be estimated to be approximately equal to 3.5 times the length of the half-diagonal of the indentation. The penetration depth of the indenter is in the range of 0.45–0.55 μm for most measurements. Therefore, the length of the diagonal is in the range of 3–4 μm and the resulting radius of the plastic zone is in the range from 5 to 7 μm. In this ideal picture, the number of particles in the plastically deformed volume, for an uniform distribution of spherical particles of 1 μm diameter and 3% carbon volume fraction, can be estimated to be in the range from 15 to 40 (this would be about 10 for 1.0% carbon volume fraction), that is a relatively large number that may account for a short interparticle distance. In this frame, also the low reproducibility of microhardness values for composite coatings prepared from baths not subjected to UST can be reasonably explained. In fact, if we accept the view that the characteristics of the UDD suspension (size and size distribution of aggregates in the composite bath) may change significantly from one single bath to the other, when UST is not applied, size and distribution of embedded UDD particles and aggregates can be expected to change locally in an unpredictable way. This would explain why we observed low reproducibility of microindentation data for samples obtained from several baths without UST having the same composition and under nominally the same operative conditions. Moreover, size distribution of particles and aggregates could as well affect some microstructural features of the matrix, such as grain size and preferred orientation, thus exerting an additional influence on mechanical properties.

The sliding wear rate of composite coatings is also substantially improved compared to the pure Au matrix, most likely as a consequence of reduced adhesion wear, as can be expected as a result of both matrix strengthening and reduced contact between the mating metal surfaces. Moreover, at least for composite layers from bath subjected to UST, there was no evidence of abrasive wear enhancement of Au/n-C(A4) composite coatings.

Conclusion

Gold / nanosized diamond composite coatings were successfully prepared from a sulphite based gold electrolyte with the main objective of improving noteworthy critical properties of such gold coatings, that is mechanical strength and wear resistance. Even very low volume fraction of embedded particle shows remarkable effects of matrix strengthening preserving very high caratage. Further studies are under way in order to improve process control and properties reproducibility

in view of application such as electroforming and generally thick coatings deposition.

Acknowledgements We would like to thank Prof. Luca Nobili for helpful discussions during the revision of the paper. The authors are indebted to Dr. G. Angella, CNR - IENI, Milano, for TEM imaging of UDD nanoparticles. We also acknowledge support from Ministero dell'Istruzione, dell'Università e della Ricerca MIUR under project PRIN 2002.

References

1. Celis JP, Roos JR (1982) Rev Coat Corr 5:1
2. Feldstein N (1990) Composite electroless plating in electroless plating: fundamentals and applications. In: Mallory GO, Hajdu JB (eds), William Andrew Publishing/Noyes, p269
3. Hovestad A, Janssen LJJ (1995) J Appl Electrochem 40:519
4. Stojak JL, Fransaer J, Talbot JB (2002) Review of electrocodeposition in advances in electrochemical science and engineering. In: Alkire RC, Kolb DM (eds) Wiley VCH, Germany, Vol.7, p193
5. Greco VP (1989) Plat Sur Finish 76(10):68
6. Verelst M, Bonino JP, Rousset A (1991) Mater Sci Eng A 135:51
7. Bozzini B, Giovannelli G, Boniardi M, Cavallotti PL (1999) Comp Sci Techn 59:1579
8. Bozzini B, Martini C, Cavallotti PL, Lanzoni E (1999) Wear 806:225
9. Rashkov S, Atanassov N (1980) J Appl Electrochem 10:535
10. Strudel JL (1996) Mechanical properties of multiphase alloys in physical metallurgy. Cahn RW, Haasen P (eds) Cambridge University Press, IV Ed., Vol.3, p2114
11. Greco VP (1989) Plat Sur Finish 76(7):62
12. Garcia I, Fransaer J, Celis JP (2001) Surf Coat Technol 148:171
13. Zimmerman AF, Palumbo G, Aust KT, Erb U (2002) Mater Sci Eng A 328:137
14. Qu NS, Chan KC, Zhu D (2004) Scripta Mat 50:1131
15. Larson C (1984) Gold Bull 17(3):86
16. Musiani M (2000) Electrochem Acta 45:3397
17. Buelens C, Celis JP and Ross JR (1983) J Appl Electrochem 13:541
18. Buelens C, Celis JP, Roos JR (1985) Trans IMF 63:6
19. De Bonte M, Celis JP and Roos JR (1992) In: Eugen G (ed) Precious metals-modern technologies and application east report 1991, Leuze Verlag, Saulgau/Württ, p81
20. Zielonka A, Fauser H (1999) Zeitschrift fur Physikalische Chemie 208:195
21. Serhal Z, Morvan J, Berçot P, Rezrazi M, Pagetti J (2001) Surf Coat Technol 145:233
22. Serhal Z, Berçot P, Morvan J, Rezrazi M, Pagetti J (2002) Surf Coat Technol 150:290
23. Rezrazi M, Doche ML, Berçot P, Hihn JY (2005) Surf Coat Technol 192:124
24. Bollini G, Bozzini B, Giovannelli G, Cavallotti PL (1996) AIFM Galvanotecnica Nuove Finiture 6(1):22
25. Bozzini B, Cavallotti PL (2001) Praktische Metallographie 38:88
26. Boniardi M, Bozzini B, Giovannelli G, Cavallotti PL (1999) Composit Sci Technol 59:1579
27. Bozzini B, Giovannelli G, Cavallotti PL (1999) J Appl Electrochem 29:685
28. Bozzini B, Giovannelli G, Cavallotti PL (2000) J Appl Electrochem 30:591
29. Cojocaru P, Ciucci F, Vicenzo A, Cavallotti PL (2004) In Atti 30° Convegno Nazionale AIM
30. See: http://www.nanodiamond.com
31. Piontelli R, Poli G, Serravalle G (1959) In : Yeager E (ed) Transactions of the symposium on electrode processes. Wiley, p67. Piontelli R (1966) Electrochim Metall 1:5
32. Dolmatov Yu V (2001) Russ Chem Rev 70:607
33. Derivaz J-P, Resin A, Losi S (1977) Surf Technol 5:369
34. Wünsche F, Bund A, Plieth W (2004) J Solid State Electrochem 8:209
35. Wang L, Gao Y, Huiwen L, Xue Q, Xu T (2005) Surf Coat Technol 191:1
36. Loubnin EN, Pimenov SM, Blatter A, Schwager F, Detkov PY (1999) New Diamond Front Carbon Technol 9(4):273
37. Dolmatov VY (1998) J Superhard Mater 20(4):70
38. Guglielmi N (1972) J Electrochem Soc 119:1009
39. Müller B, Ferkel H (1998) NanoStructured Mat 10:1285
40. Johnson KL (1985) Contact mechanics. Cambridge University Press, Cambridge, p172